THESIS FOR THE DEGREE OF LICENTIATE OF ENGINEERING

Modeling of the wet-out process in composites manufacturing

DA WU

Department of Industrial and Materials Science
Division of Material and Computational Mechanics
CHALMERS UNIVERSITY OF TECHNOLOGY

Gothenburg, Sweden 2018

Modeling of the wet-out process in composites manufacturing
DA WU

Thesis for the degree of Licentiate of Engineering
Department of Industrial and Materials Science
Division of Material and Computational Mechanics
Chalmers University of Technology
SE-412 96 Gothenburg
Sweden
Telephone: +46 (0)31-772 1000

Cover:
Snapshot from a simulation of a liquid composite molding process. The liquid resin is transferring in a deformable fiber preform. The contour shows the degree of saturation and the arrows indicate the flow directions.

Chalmers Reproservice
Gothenburg, Sweden 2018

Modeling of the wet-out process in composites manufacturing
Thesis for the degree of Licentiate of Engineering
DA WU
Department of Industrial and Materials Science
Division of Material and Computational Mechanics
Chalmers University of Technology

Abstract

The fiber reinforced polymer composites (FRPCs) are carving out a niche amid the keen market competition to replace the other material counterparts, e.g., metals. Due to the low weight and corrosion resistance, the FRPCs are wildly utilized from aviation to automobile industries; both in the sectors of civilian and defense. To obtain high-quality products at low cost, the composite industry continues seeking numerical simulation tools to predict the manufacturing processes instead of prototype testing and trials. Regarding the attractive liquid composite molding (LCM) process, it provides the possibility to produce net shape parts from composites. The main focuses are of the simulation efforts of the flow in the mold and the deformation of fiber networks for optimizing and improving manufacturing processes.

Concerning the modeling, one potential interest is to describe physics at the macroscopic level. Then, the theory of porous media (TPM), which relies on the concept of volume fractions, can explain the liquid saturated multiphase materials considerably. The Darcy's law describes the relation between the flow velocity and the pressure gradient, without accounting for the microscale flow and fiber bundles coupling. Combining with the mass conservation principle, we can develop the numerical method to simulate the flow during wetting and drying processes. To this end, the gas and liquid resin compose the homogenized flow in the model. Unlike the traditional models that ignore the role of gas flow, the new model introduces the capillary effect and the relative permeability to achieve a better free surface flow front tracking. What's more, the mechanism that the gradient of saturation degree also contributes to the flow velocity is revealed herein, and an extension of Darcy's law is derived as well.

As to the other phenomenon, e.g., fiber networks compaction and thickness variations, it is possible to use the Terzaghi effective stress principle and the packing law from Staffan Toll to model those issues. A normal directional stretch kinematic assumption is developed to reduce the model from full 3-D to a shell-like problem. Given this, an explicit formulation is obtained to express the normal directional stretch as a function of homogenized flow pressure. By embedding the flow into the shell-like fiber network, we end with a non-linear coupled equation system that solves for the homogenized flow pressure, the saturation degree and the normal directional stretch. The finite element method is employed to solve equations with the staggered approach, especially the Streamline-Upwind/Petrov-Galerkin method is employed to eradicate the stability problems.

Keywords: liquid composite molding, porous media theory, process modeling, free surface flow, fiber preform deformation

燦燦萱草花　羅生北堂下
南風吹其心　搖搖為誰吐
慈母倚門情　遊子行路苦
甘旨日以疏　音問日以阻
舉頭望雲林　愧聽慧鳥語
墨萱圖　王冕

Preface

The work in this thesis was carried out from September 2015 to May 2018 at the Division of Material and Computational Mechanics, Department of Industrial and Materials Science, Chalmers University of Technology. The research was financially supported by the Swedish Research Council (Vetenskapsrådet) grant no. 621-2013-3907. Some of the numerical simulations presented herein were performed on resources at the Chalmers Centre for Computational Science and Engineering (C3SE) provided by the Swedish National Infrastructure for Computing (SNIC).

Acknowledgements

Firstly, I would like to express my sincere gratitude to my supervisor Prof. Ragnar Larsson for the continuous support of my Ph.D. study and related research, for his patience and immense knowledge. I could not imagine having a better advisor and mentor for my Ph.D. study.

I thank my colleagues and friends at the divisions of Dynamics, Material and Computational Mechanics. For the stimulating discussions, for all the fun we have had in the past years, for enlightening me the first glance of research, and for the rewarding workplace.

I especially thank Dr. Mohammad S. Rouhi and Dr. Maciej Wysocki for their previous contributions. I also want to thank Prof. Leif Asp and all composite group-mate for constructive suggestions in meetings. Moving on, I would like to express my appreciation to Prof. Magnus Ekh, for sharing his knowledge of mechanics with me. I thank Mr. Adam Ścięgaj for his information about how to "do the licentiate degree right". Of cause, Mr. David Carlstedt, my roommate, I thank you for letting me use my "twittering" mechanical keyboard inside the office to write this thesis without any noise complaint. I still want to thank Mr. Senad Razanica, who always gives me a free ride.

Last but not the least, I would like to thank my parents, my dearest wife, Maria, and her parents for supporting me spiritually throughout my life. Wish all our dreams come true!

Göteborg, May 2018

Da Wu

Thesis

This thesis consists of an extended summary and the following appended papers:

Paper A	Da Wu, Ragnar Larsson "Homogenized free surface flow in porous media for wet-out processing" *International Journal for Numerical Methods in Engineering* (2018). ISSN: 00295981. DOI: 10.1002/nme.5812
Paper B	Da Wu, Ragnar Larsson "Modeling of the planar infusion flow in deformable thin-walled composite components" *To be submitted for publication*

The appended papers were prepared in collaboration with the co-authors. The author of this thesis was responsible for the major progress of the work in the papers, i.e., took part in formulating the theory, led the planning of the papers, developed the numerical implementation, carried out the numerical simulations, and prepared the manuscript.

Contents

Part I
Extended Summary

1 Introduction

1.1 Background

Since the early 1980s, the human-made composite materials have been introduced in the aviation industry. Especially the fiber reinforced polymer composites (FRPCs) have advantages, e.g., low weight, corrosion resistance, and high stiffness and strength. With this attractive properties, the FRPCs utilization is widely spread among the transportation industry, the energy industry, and sports technology, and the list goes on. The aerospace industry even uses the “black aluminum” to name the FRPCs, since the FRPCs are “lighter than aluminum and stronger than steel”. All of the above reasons accelerate the replacement of metal counterparts, for energy savings, durability, and life-cycle enhancement. For instance, Boeing and Airbus keep pushing the composites intensively into their final products, e.g., composite materials contribute over 50% airframe weight in both 787 and A350 [22].

However, it is still expensive to use FRPCs in the high-rate productions. The costs of raw material and manufacturing process contribute primarily. The out-of-autoclave cure (OAC) processes can promise the manufacturing cost reduction. Unlike the autoclave cure process, the OAC process allows more massive throughput and lean production initiatives. The resin transfer molding (RTM) and vacuum-assisted resin transfer molding (VARTM) are typical OAC processes. Both RTM and VARTM are parts of the liquid composite molding family, which have been extensively utilized to produce large-scale products, e.g., wind turbine blades, posts and ship hulls.

On the other hand, the advanced simulation CAE tools are also critical drivers for the cost reduction. CAE tools help engineers to reduce the design cycle time. Furthermore, before the pilot production, the manufacturing feasibility test can be checked through simulations, and the massive cost will be saved compared with expensive prototype trials.

To model and simulate the FRPCs manufacturing processes, two prime tasks can be addressed: i) the free surface flow modeling and ii) the fiber preform modeling. Regarding the flow modeling, various approaches are focusing on the detailed seepage in porous materials, e.g., the hybrid mixture theory [30], the thermodynamically constrained averaging theory [24] and the theory of porous media. The mass conservation equations can be formulated based on those theories, and be solved with different methods. For instance, the most common control volume finite element method (CVFEM), and using the volume of fraction (VOF) for tracking the flow front locations, e.g., [10, 58, 62, 39, 32, 41, 49, 61, 68]. Also, the boundary element method (BEM) can be employed to trace the flow motion, e.g., [29, 59]. Furthermore, the level set method [53] and the meshless method, e.g., smoothed particle hydrodynamics (SPH) [6, 50, 13] are lately exhibited. Recent natural element method (NEM) [40] and discontinous Galerkin method (DGM)

[47] are developed to improve the flow front tracking.

Instead of only focusing on the single-phase fluid, e.g., [11], the gas-liquid mixed fluid is also attractive, e.g., the three-phase porous media models [18, 28, 48, 43] account for the integration of gas, liquid resin, and solid fiber networks. Further, as [64] suggests, the gas and liquid phases can be treated as homogenized flow then embedded into fiber networks.

On the other hand, Li and Tucker [31] report a particular anisotropic, hyperelastic constitutive relation to model the solid stress response. Besides, Wysocki, Larsson, and Toll work on the fiber preform modeling, e.g., [57, 27, 66, 65, 67], whose works focus on the consolidation and fiber preform thickness variation. The above studies are based on the assumption that resin surrounds the fiber bundles, and the hydrostatic pressure governs the deformation, viz., hydrostatic consolidation. However, those studies are either limited to 2-D problems or require high computational efforts for 3-D full space cases. So it is attractive to develop a computation efficient multi-phase porous media model to simulate both flow front positions and fiber preform response, for instance, the model of the wet-out process in composite manufacturing.

1.2 Aim, scope and limitations

The purpose of this thesis work is to develop a mathematical model for simulating the wet-out process during the composite manufacturing. To this end, some research objectives are listed as follows:

- introduce the gas phase and the relevant capillary effect into the previous framework, develop a three-phase porous media model;
- use feasible stabilized finite element methods to solve the problem, obtain reasonable flow fronts;
- develop a shell-like model for describing the fiber networks swelling and compaction;
- reduce the model from 3-D to 2-D.

In addition to the above list, the justification of the model accuracy and the performance examination is also imperative to carry out.

The work is limited to model the liquid composite molding (LCM) process at the macroscopic level. The fluid-solid interaction is based on the theory of porous media, plus the limited low flow rate. The microscale fiber structures and the microflow in the vicinity of the fiber bundles are not considered herein. The current study focuses on the isothermal condition, and the sources and sinks are ignored when formulating the mass conservation equations. In addition, the preform is modeled hyperelastic, and before failure.

2 Composites manufacturing process

The fiber reinforced polymer composites (FRPCs) consist of fibers in polymer matrices to combine the benefits of both fiber and polymer properties while getting rid of their shortcomings. The fiber can be either short or continuous, and the polymer matrices can be thermoset or thermoplastic. The challenge of short-fiber composites production is the density distribution and fiber orientation, which give rise to the inhomogeneous performance products. On the other hand, regarding the continuous fiber FRPCs, the bad fiber-matrix interfacial bounding due to the incomplete filling may lead to the initial delamination and cracks. To fabricate the short-fiber composites, one can choose the injection and compression molding processes, or the state-of-art polymer matrix nanocomposites process. As to the continuous fiber FRPCs, the pultrusion process and continuous compression molding (CCM) process are wildly utilized in the industry. When it is required to produce net shape and large-scale components, the liquid composite molding process (LCM) is attractive.

The LCM is a large family of processes. Generally, the concept of LCM process is to transfer the liquid resin from a reservoir into fiber preforms that are placed in a cavity mold. The fiber preform can be among types of woven, non-crimp, random mat and bidirectional fabrics. The thermoset polymer has low viscosity and usually chosen for the processing. The resin transfer molding (RTM) is the first member of the LCM family. This method is easy to use to produce load-bearing composite components. During the last couple decades, many types of research have been done to study the physics of the process and develop the numerical and experimental models, cf. [1, 45, 15, 36, 35, 38, 60, 37, 34]. The vacuum-assisted resin transfer molding (VARTM) is a variation of the RTM. It is invented for cost consideration. VARTM can be used to produce large-scale composite structures. Instead of using a rigid cover mold, a vacuum bag is used to seal the model and preform. An improved Seemann's composites resin infusion molding process (SCRIMP) [51, 52] is developed based on VARTM. It has short filling time comparing with VARTM process. Moreover, there are other members of the LCM family, for instance, the compression resin transfer molding (CRTM) process, the resin infusion under flexible tooling (RIFT), the RTM Light, the resin film infusion and vacuum injection preform relaxation (VIPR), cf. [4]. Although the LCM processes are hot methods among many industries nowadays, e.g., wind power, marine, and vehicle, the high volume production is difficult because of the intensive workloads and lack of automating streamlines.

There is a type of process suits for the fabrication of high performance and sophisticated shape composite components. The autoclave processing uses the autoclave to provide high pressure and temperature environment to help to control the products quality, e.g., volume fraction, residual stress, and final shape. Many researcher, e.g., cf. [55, 1, 69, 70, 41] put efforts to investigate the science base of this process, and suggests different models to improve the design of processing.

Due to the high cost of the autoclave and also the extensive safety regulations for operating, the out-of-autoclave (OoA) class of process is introduced. For example, the vacuum bag only OoA (VBO-OoA) process represents the latest OoA curing techniques. Besides the processes mentioned above, [5, 3, 55, 26, 25] mention other types of process, which can be referred as further information.

2.1 Resin transfer molding process

Since the mid-1980s, the resin transfer molding (RTM) process have developed during the last two decades. It can be utilized to produce high volume fraction net shape FRPCs components. It was first adopted in the automotive industry. The continuous fiber networks, e.g., woven and stitched preform are placed in a net-shaped mold, filled by high-pressure resin flow, which grantees good mechanical properties and qualities.

Figure 2.1 shows typical RTM process steps. First, the fabric plies are draped on the mold surface. While draping, the fabric plies may be glued with the tackifier to keep bounding during the infusion stage. Secondly, the mold is closed by a rigid cover and clamped. Now the injection is started, the resin is injected into the fiber preform under positive pressure. At the moment resin flow out the vents, the infusion process is cut off, and let the resin cure. At this stage, the mold could be heated up as resin curing demands. Until the consolidation of resin is finished, the mold is ready to open.

To overcome various issues of RTM process, the composite material manufacturers developed many variational processes. For large-scale FRPCs fabrication, the vacuum assisted resin transfer molding (VARTM) and the Seemann's composites resin infusion molding process (SCRIMP) inherit from RTM. The modified VARTM, vacuum-induced preform relaxation (VIPR) reduces the fill time. The fast remotely actuated channeling (FASTRAC) can create temporary race-tracking channels to accelerate the process comparing with RTM. There are still other modified versions, e.g., light RTM (LRTM), structural reaction injection molding (S-RIM), co-injection resin transfer molding (CIRTM), compression resin transfer molding (CRTM) and resin infusion between double flexible tooling (RIDFT), which are further described in [5, 3, 55, 26, 25].

The advantages of the RTM process are listed as follows, cf. [2]:

- The final products are net-shaped with the good finish surface and fine dimensional tolerances.
- Manufacturing complex geometries are feasible.
- Manufacturing high volume fraction composites are available, because of high compaction pressure.
- The finish products usually have high mechanical properties and can be used as load-bearing components.
- The manufacturing rate is high due to 1) high injection pressure and 2) automation is available.

The disadvantages are summarized as follows:

- The variations of preform due to the inconsistent of fabric cutting, draping, pre-impregnating.
- The dimensions are limited due to the constrained mold size.

- The dry spots are sensitive to the gating and venting placements.
- The high flow pressure can cause fiber washing due to loose compaction.

2.2 Vaccum assisted resin transfer molding process

The vacuum assisted resin transfer molding process belongs to the type of closed-mold method, which can be used to manufacture large-scale FRPCs. The process inherits the advantages of RTM, e.g., low volatile organic compounds emission, high quality, and clean operating environment. Also, this process method is flexible and scalable, and usually, the tooling cost is low.

A feature of the VARTM is that the preform is closed by the easily deformed semi-permeable membrane and compressed by the atmospheric pressure. The preform is assembled as a sandwich that consists of fiber networks, peel ply, flow distribution media and helical tubes. Due to this low-pressure requirement, the VARTM process can be operated like the open mold process, and consequently allows one-piece large-scale structures. A significant difference between RTM and VARTM is the injection pressure. In the RTM process, because of the rigid mold cover is strong enough, the injection pressure can be dramatically higher than the environmental pressure, which leads to a positive pressure environment inside the mold cavity. However, this is not feasible in

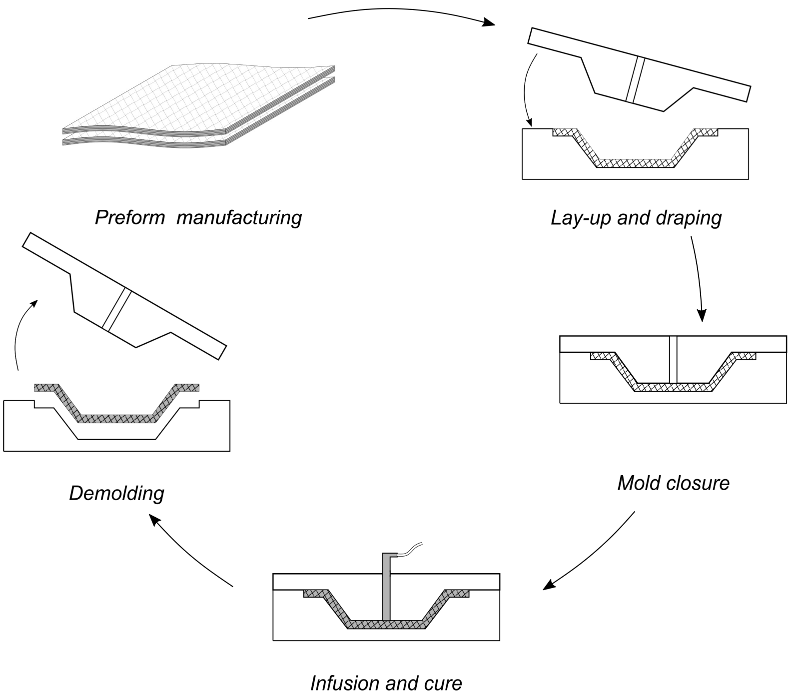

Figure 2.1: An illustration of RTM process steps

the VARTM process. The injection pressure in VARTM process usually equals to 1 atm, so the pressure difference is contributed from the internal mold vacuum. This vacuum environment will compress the preform to the lower mold and drives the resin transfer into the preform.

Figure 2.2 illustrates the VARTM process briefly, regarding the detailed steps, e.g., cf. [2]. Concerning the large or complex shape components and long time filling, the lower mold can be heated for controlling the resin viscosity and managing curing cycle (as OoA process desires). What's more, the resin inlets and outlets should be adjusted to generate versatile resin flow paths for better infusion quality and faster filling time.

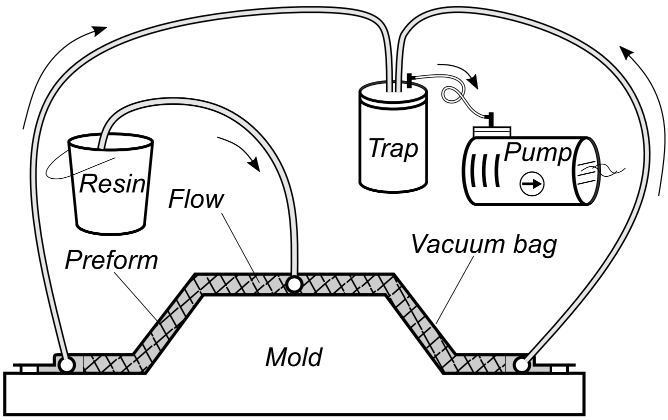

Figure 2.2: An illustration of VARTM process

Nowadays, the VARTM processes are widely employed in various types of industry, e.g., energy, infrastructure, maritime, aviation, and vehicle. It is because the advantages listed as follows cf. [2]:

- The cost of mold tooling is low, and it is flexible to design the mold tooling.
- Manufacturing complex and large-scale geometries are feasible.
- Neat operating environment due to 1) separately stored resin and catalyst and 2) low VOC emission.
- The dry spots can be easily monitored through the transparent membrane and can be fixed by adding outlets.

The disadvantages are summarized as follows:

- The high cost of the membrane, peel ply, sealing tape and tube since they are not reusable.
- High demanding on the operator's skill, to avoid air leakage.
- The injection pressure is low, which causes a long filling time.

- The fiber volume fraction is limited because of the low compressive pressure.
- It is difficult to apply automation in the process, and the workloads are high.
- The spring-in, dry spot, and microvoids may influence the products' quality.

3 The theory of porous media

3.1 The early eras

October 1760, Euler [19] gave his clear description on the *impenetrability* of a porous body – the water-saturated sponge. After that, Euler completed the theory of ideal fluids consists of continuity and motion equations during the 1770s. Reinhard Woltman [63] built a systematical soil mechanics and porous bodies framework and introduced the essential concept,*volume fraction*. Those works are known as the prerequisites for developing the porous media theory.

After Woltman's concept of volume fractions, around the mid-19th, the mixture theory and the porous bodies theory were developed significantly. Delesse's concept of surface fractions [17] became the most fundamental contribution to the porous media theory. Then the first phenomenological mixture theory was done by Fick [20]. Fick's contribution was Fick's first and second diffusion law. In 1856, Darcy [14] reported the essential study on the interaction between constituents of a multiphase continuum media, viz., Darcy's law,

$$Q = -\frac{KA(p_b - p_a)}{L} \ , \tag{3.1}$$

where Q is the instantaneous fluid discharge rate through the porous media, and K is a constant representing the porous media permeability and fluid viscosity. Josef Stefan [54] for the first time derived the motion and mass balance equations for a mixture of two gases following the continuum mechanics framework and the concept of volume fraction with the consideration of the porosity of the porous solid. This work gives the foundation of the mixture theory, and it becomes the symbol of the classical era of the development of the porous media theory.

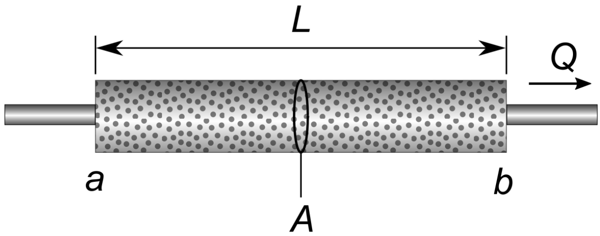

Figure 3.1: Darcy's law test

In regard to what has been achieved in the 19th century, the theory of porous media had sound background materials to usher in. During this period, the uplift, friction, *capillarity* and *effective stresses* in both liquid-saturated rigid and deformable porous solids were studied by two remarkable scientists viz., Paul Fillunger and Karl Von Terzaghi. The famous effective stress that is defined by Terzaghi shows

$$\sigma = \bar{\sigma} - p\mathbf{1} \ , \tag{3.2}$$

where $\bar{\sigma}$ denotes the effective stress, and σ is the total stress, and the p is the hydrostatic pressure of the fluid. The interesting thing is that Terzaghi developed porous media theories intuitively, not following mechanics, but rather from experiments. Then the theory continued its development by Maurice Biot, who gave the tremendous contributions to the theory, which are still cited by today's researchers. Goodman and Cowin [21] introduced an expression of the incompressibility condition of the solid material as:

$$n^s J_s = n_0^s \ , \tag{3.3}$$

where n_0^s is the solid phase volume fraction in the reference configuration, and J_s denotes the determinant of the deformation gradient of the solid. On the other hand, Morland [42], Bowen [8, 9], Nunziato [46], Boer and Ehlers [16] had studied various porous media problems and promoted the mixture theory.

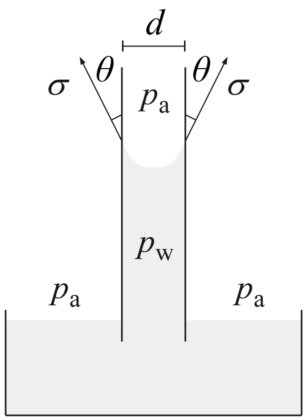

Figure 3.2: The capillary rise is due to the surface tension between gas and liquid phases. The capillary pressure in a narrow tube can be expressed from force equilibrium as $p^c = p^a - p^w = 4\sigma cos\theta/d$. For further discussions about the capillary effect, see [56].

3.2 Nowadays

The porous media is a kind of material that consists of solid constituents and closed or open pores. The pores can be flooded with fluids or gas and interact with the neighboring solid. Due to it is almost impossible to indicate the exact location of solid and pores, we must describe it alternately, viz., *volume fraction concept*. By doing so, the discontinuous porous media is interpreted as a smeared model. The motion, deformation, stress, pressure and other state variables are averaged statistically from the intrinsic values in the control volume. Thus, the (partial-) saturated porous media can be considered as a mixture of all constituents at a certain material position X^α (or x). With this substitute model, the continuum mechanics methods can be applied to handel the porous media problem, e.g., the mixture theory.

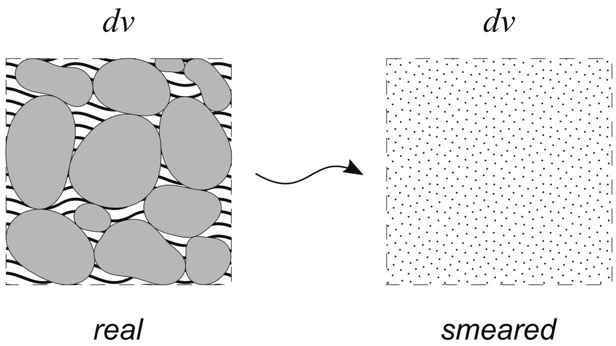

Figure 3.3: The real porous media composed of solid and liquid phases is averaged statistically to a smeared body.

Once the volume fraction concept is employed, the micromechanical effects are also "smeared" into the model. Following the porous media theory, the microscale quantities are represented by the macro-mechanical quantities instead. However, an inevitable problem is still rising: $\alpha - 1$ field equations will be missing in the α constituents porous media, i.e., the problem cannot be closed. In order to work this problem out, the microscale understanding must be included.

3.2.1 The volume fraction concept

To explain the volume fraction concept, we introduce some notations. Assuming a porous media consists of the solid phase controlling the domain B_s that bounded by ∂B_s. The v^α represents the real volumes of the constituent α among κ different constituents. In Figure 3.6, the average volume element locates at $\mathbf{x}$, $\mathbf{r}$ points the position of the α constituent that has volume dv_μ. Let's define an indicator function as

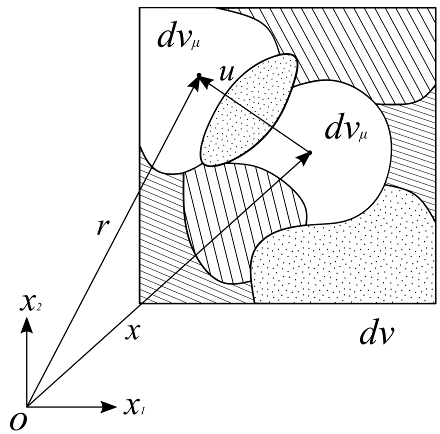

Figure 3.4: The average volume element of a multiple constituents porous media.

$$\chi^{\alpha} = \chi^{\alpha}(\mathbf{r}, t) = \begin{cases} 1 & if\ \mathbf{r} \in\ dv^{\alpha}, \\ 0 & if\ \mathbf{r} \in\ dv^{\beta}, \end{cases} \quad \alpha \neq \beta\ . \tag{3.4}$$

So the volume element of the constituent α in the total volume element can be expressed by

$$dv^{\alpha}(\mathbf{x}, t) = \sum_{i}^{\kappa} dv_{\mu}^{i} = \int_{dv} \chi^{\alpha}(\mathbf{r}, t)\, dv_{\mu}\ . \tag{3.5}$$

Now we can formulate the volume fraction as

$$n^{\alpha}(x, t) = \frac{1}{dv} \int_{dv} \chi^{\alpha}(r, t)\, dv_{\mu} = \frac{dv^{\alpha}}{dv}\ , \tag{3.6}$$

with the constraint,

$$\sum_{i=1}^{\kappa} n^{i} = 1. \tag{3.7}$$

If the real or intrinsic density of α constituent at location r can be defined as $\rho^{\alpha\mathbf{r}} = \rho^{\alpha\mathbf{r}}(\mathbf{r}, t)$, thus the real density at the x yields $\rho^{\alpha\mathbf{x}} = \rho^{\alpha\mathbf{x}}(\mathbf{x}, t)$, and of cause the macroscale quantity is $\rho^{\alpha} = \rho^{\alpha}(\mathbf{x}, t)$. Now we can obtain two critical relations of the density form the volume fraction concept

$$\rho^{\alpha\mathbf{x}}(\mathbf{x}, t) = \frac{1}{dv^{\alpha}} \int_{dv} \rho^{\alpha\mathbf{r}}(\mathbf{r}, t)\, \chi^{\alpha}(\mathbf{r}, t)\, dv_{\mu} = \rho^{\alpha\mathbf{r}}(\mathbf{r}, t)\, \frac{dv^{\alpha}}{dv^{\alpha}} = \rho^{\alpha\mathbf{r}}\ , \tag{3.8}$$

and

$$\rho^{\alpha}(\mathbf{x}, t) = \frac{1}{dv} \int_{dv} \rho^{\alpha\mathbf{r}}(\mathbf{r}, t)\, \chi^{\alpha}(\mathbf{r}, t)\, dv_{\mu} = \rho^{\alpha\mathbf{r}}(\mathbf{r}, t)\, \frac{dv^{\alpha}}{dv} = n^{\alpha}(\mathbf{x}, t)\rho^{\alpha\mathbf{r}}\ . \tag{3.9}$$

3.2.2 Kinematics

In order to address the kinematics of the porous media theory, we need to make two certain assumptions:

- At a certain time t, all of the constituents share the same spatial point $\mathbf{x}$, but the trajectories are from different reference configurations at $t = t_0$;
- thus, every constituent in the heterogeneous mixture has an independent motion.

Based on these assumptions, we define the deformation mapping following the continuum mechanics framework,

$$\mathbf{x} = \varphi^{s}(\mathbf{X}^{s}) = \varphi^{f}\left(\mathbf{X}^{f}\right)\ ,\ \mathbf{X}^{s} \neq \mathbf{X}^{f}\ , \tag{3.10}$$

where φ^{s} and φ^{f} represent the deformation mapping of the solid and fluid phases respectively. Thus the corresponding deformation gradient can be defined as

$$\mathbf{F}^{\alpha} = \varphi^{\alpha} \otimes \nabla_{\mathbf{X}}\ . \tag{3.11}$$

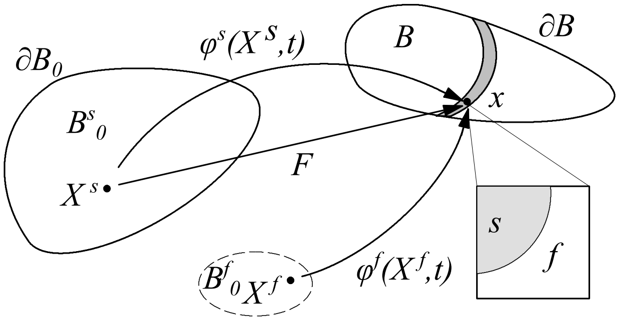

Figure 3.5: The motion of the solid and fluid phases for a saturated porous media.

Moreover, the Jacobian J^α can be obtained as

$$J^\alpha = \det(\mathbf{F}_\alpha) > 0 \ . \tag{3.12}$$

Next, the velocity of each constituents can be defined as

$$v^\alpha = (\dot{\mathbf{x}})_\alpha = \frac{D^\alpha \varphi^\alpha(X^\alpha)}{Dt} = \dot{\varphi}^\alpha(X^\alpha) \ , \tag{3.13}$$

where the operator $(\dot{\bullet})_\alpha$ denotes the material time derivative for the reference configuration of the constituent α.

From the definition, we know the intrinsic velocity of the constituent α. In order to include the velocity in the constitutive relation – Darcy's law, we need a relationship between the intrinsic velocity and Darcy's velocity. Let f_w represent the area of a cross-section of a cylinder where the fluid can pass through (refer to Figure 3.1). Thus we obtain $Q = f_w v^f$, where f_w also denotes the porosity on the cross-section. From Deless [17], we notice that the surface porosity equals to the volume porosity, i.e., $f_w = n^f$. Finally, we conclude,

$$Q = v^{df} = n^f v^f. \tag{3.14}$$

3.2.3 Mass balance

In this section, we consider the mass balance for the individual constituent α. The mass balance can be express by words as – the rate of change of the mass M^α is equal to the mass supply $\int_{B_\alpha} \hat{\rho}^\alpha dv$, where $\hat{\rho}^\alpha$ denotes the density supply. The formulation reflects,

$$(\dot{M}^\alpha)_\alpha = \overline{\left(\int_{B_\alpha} \rho^\alpha dv\right)}^{\,\cdot}_\alpha = \int_{B_\alpha} \hat{\rho}^\alpha dv \tag{3.15}$$

From the fundamental continuum mechanics knowledge, we conclude the mass balance equation for single phase α

$$\frac{\partial \rho^\alpha}{\partial t} + \operatorname{div}(\rho^\alpha \mathbf{v}^\alpha) = \hat{\rho}^\alpha. \tag{3.16}$$

If using a homogenized velocity $\mathbf{v}$ substitute the intrinsic velocity $\mathbf{v}^\alpha$ of each constituent, we obtain a mass balance equation for the bulk heterogenous mixture

$$\sum_{\alpha=1}^{\kappa}\left[\frac{\partial\rho^\alpha}{\partial t}+\operatorname{div}\left(\rho^\alpha\mathbf{v}\right)\right]=\sum_{\alpha=1}^{\kappa}\hat{\rho}^\alpha\ . \tag{3.17}$$

As it is mentioned previously, the problem is not closed. For a two-phase porous media problem, we introduce an auxiliary equation from the constraint (3.7) to close the problem

$$(\dot{n^s})_s+(\dot{n^f})_s=0\ , \tag{3.18}$$

and

$$-(\dot{n^s})_s-(\dot{n^f})_f+\operatorname{grad}n^f\cdot\mathbf{v}^r=0\ , \tag{3.19}$$

where $\mathbf{v}^r=\mathbf{v}^f-\mathbf{s}^s$ is the relative velocity.

Until now, we have a closed mass balance equation system for the two-phase (solid and fluid) porous media problem. If the fluid phase consists of gas and liquid, we introduce a homogenization routine to consider the gas and liquid phase as a mixed fluid phase to reduce the complexity of the problem.

Let ξ represents the degree of saturation, we have

$$n^f=\phi^l+\phi^g=\xi n^f+(1-\xi)n^f\ , \tag{3.20}$$

where $\phi^l=\xi n^f$ is the volume fraction of the liquid phase, and $\phi^g=(1-\xi)n^f$ is the volume fraction of the gas phase. Applying the volume averaging on the density of both phases, we obtain the mixture fluid homogenized density as

$$\rho^f=\xi\rho^l+(1-\xi)\rho^g\ , \tag{3.21}$$

and the mixture pressure as

$$p^f=\xi p^l+(1-\xi)p^g\ . \tag{3.22}$$

From Figure 3.2, we know that $p^c(\xi)=p^g-p^l$, which is derived by Gray and Hassanizadeh [23]. Thus we build a connection between the liquid and gas pressure as

$$p^l=p-(1-\xi)p^c(\xi)\ ,\quad p^g=p+\xi p^c(\xi)\ . \tag{3.23}$$

Combing Darcy's law and the results form homogenization, we can derive Darcy's velocity of the mixture fluid in a mixture fashion,

$$\mathbf{v}^{df}=\frac{\rho^l}{\rho^f}\mathbf{v}^{dl}+\frac{\rho^g}{\rho^f}\mathbf{v}^{dg}\ . \tag{3.24}$$

If we choose the ξ and p as primer variables to solve, a modified fluid Darcy's velocity expression can be obtained

$$\mathbf{v}^{df}=-K_1\nabla p-K_2\nabla\xi\ , \tag{3.25}$$

where K_1 and K_2 are homogenized permeabilities. Using these results in the mass balance Equation 3.16 and 3.17, we can conclude a close mass balance system for three-phase porous media problem. The closed system then can be used to track the flow front, e.g., to predict the resin flow during the wet-out processing in the composite material manufacturing, cf. [64].

3.2.4 Balance of momentum

The balance of momentum tells that the rate of change of the linear momentum equals to the sum of resultant force if the density supply is ignored, the formulation shows

$$\overline{\left(\int_{B_\alpha} \rho^\alpha \mathbf{v}^\alpha dv \right)}^{\cdot}_{\alpha} = \int_{B_\alpha} (\rho^\alpha \mathbf{b}^\alpha + \hat{\mathbf{p}}^\alpha)\, dv + \int_{\partial B_\alpha} \mathbf{t}^\alpha ds \;, \tag{3.26}$$

where $\rho^\alpha \mathbf{b}^\alpha$ is the body force, $\hat{\mathbf{p}}^\alpha$ is the interaction force, and $\mathbf{t}^\alpha$ is the surface traction. Given Cauchy's law and the divergence theorem, the balance of momentum for the α phase is formulated as

$$\operatorname{div} \boldsymbol{\sigma}^\alpha + \rho^\alpha \mathbf{b}^\alpha + \hat{\mathbf{p}}^\alpha = \rho^\alpha (\dot{\mathbf{v}^\alpha})_\alpha \;. \tag{3.27}$$

If the common velocity $\mathbf{v}$ and acceleration $\mathbf{b}$ are introduced, the momentum balance for the whole mixture bulk body can be expressed as

$$\sum_{\alpha=1}^{\kappa} (\operatorname{div} \boldsymbol{\sigma}^\alpha + \rho^\alpha \mathbf{b} + \hat{\mathbf{p}}^\alpha) = \sum_{\alpha=1}^{\kappa} \rho^\alpha \dot{\mathbf{v}} \;. \tag{3.28}$$

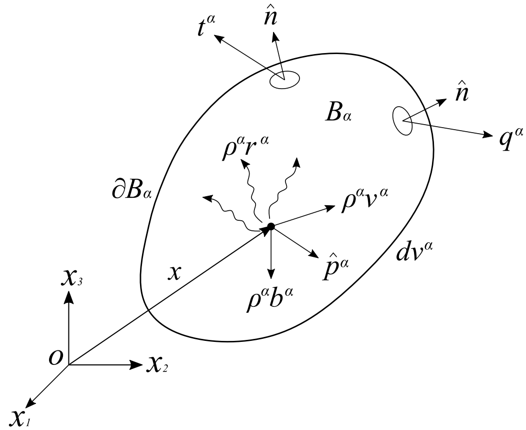

Figure 3.6: Continuum in motion for α phase.

3.2.5 Energy balance

The first law of thermodynamics justifies the energy balance, which tells that the rate of change of internal and kinetic energies is balanced by the mechanical power and the thermal power. For an individual constituent α in the porous media, let E, K, W and Q represent internal energy, the kinetic energy, the mechanical power and the thermal power respectively, the balance of energy can be formulated as

$$(\dot{E^\alpha})_\alpha + (\dot{K^\alpha})_\alpha = W^\alpha + Q^\alpha \;. \tag{3.29}$$

After some derivations and using linear momentum balance, the energy balance can be reformulated as

$$\rho^\alpha (\dot{e^\alpha})_\alpha = \boldsymbol{\sigma}^\alpha : \mathbf{D}^\alpha + \rho^\alpha r^\alpha - \operatorname{div} \mathbf{q}^\alpha \ , \tag{3.30}$$

where e^α is the specific internal energy, $\mathbf{D}^\alpha$ is the rate-of-deformation tensor, r^α is the energy source, and $\mathbf{q}^\alpha$ is the heat flux. As previous approaches, let $e^\alpha = e$, $r^\alpha = r$, $\mathbf{D}^\alpha = \mathbf{D}$, and $\mathbf{q}^\alpha = \mathbf{q}$ the energy balance for the mixture porous body yields

$$\sum_{\alpha=1}^{\kappa} (\rho^\alpha \dot{e}) = \sum_{\alpha=1}^{\kappa} (\boldsymbol{\sigma}^\alpha : \mathbf{D} + \rho^\alpha r) - \operatorname{div} \mathbf{q} \ . \tag{3.31}$$

3.2.6 Entropy inequality

The second law of thermodynamics is also known as entropy principle has been used to retrieve constitutive relations since 1963 [12]. Regarding the porous media, the summation of the entropy of each constituent should always hold the principle. If the supply density $\hat{\rho}^\alpha$ is ignored, thus the local form of the entropy inequality is expressed,

$$\sum_{\alpha=1}^{\kappa} \left[\rho^\alpha (\dot{\eta^\alpha})_\alpha - \frac{1}{\Theta^\alpha} \rho^\alpha r^\alpha + \operatorname{div} \left(\frac{1}{\Theta^\alpha} \mathbf{q}^\alpha \right) \right] \geqslant 0 \ , \tag{3.32}$$

where η^α is the specific entropy, and Θ^α is the absolute temperature. In addition, the free Helmholtz energy is formulated as $\psi^\alpha = e^\alpha - \Theta^\alpha \eta^\alpha$. The further discussions about the entropy inequality and constitutive relations for porous media, see also [57, 67, 7, 27].

4 Summary of appended papers

Paper A: **Homogenized free surface flow in porous media for wet—out processing**
The paper proposes a mathematical model for simulating the wet-out processing, e.g., the infusion of the liquid composite molding process. Based on the theory of porous media, we use the concept of volume fraction to distinguish the contents of solid fiber and fluids phases. Then the saturation degree is utilized to separate the fluid as air and liquid resin. By introducing the capillary effect between gas and liquid resin phases, we employ the concept of relative permeability. It has been justified that the existing of the relative permeability plays a significant role to obtain a discontinuous like free surface front, which has been ignored in previous studies. Further, both fluid phases are homogenized as a mixture flow, characterized by the variable of mixture pressure. From the homogenization, we extend the standard Dary's law to this homogenized flow. The interest is the flow velocity not only determined by the pressure gradient only but the gradient of the saturation as well. Moreover, when the capillary effect is small enough to ignore, the extended Dary's law will turn back to the standard. The governing equations are then derived from the mass conservation principle. The saturation equation is obtained from the mass balance of the liquid resin, while the pressure equation is derived from the homogenized flow mass conservation. To solve out this high non-linear and coupled equation system, we employed the finite element method together with the staggered approach. What's more, the severe fluctuation of the saturation degree solution is noticed. The reason for this problem is because the saturation degree equation turns out to be a convection domain formulation. To enhance the stability, we adopt the Streamline-Upwind/Petrov-Galerkin (SUPG) technique in the original formulation. Finally, the model accuracy and convergence of the FE solutions are demonstrated through 1-D and 2-D examples, which represents Resin Transfer Molding processes.

Paper B: **Modeling of the planar infusion flow in deformable thin-walled composite components**
In this paper, we continuous extending the contribution from **Paper A**. The fiber preform deformation is modeled together with the flow simulation in this work. Some types of the liquid composite molding process, e.g., the vacuum assisted resin transfer molding (VARTM) process has the thickness variation problem on the final products. This is due the fiber preform deforms during the infusion process caused by the flow pressure unevenly distributed. Besides, the process like VARTM usually is used to produce large-scale composite parts, which are typically thin-walled components. Since the components are thin enough to ignore the variation of the through-thickness direction flow, we can reduce the problem from a full 3-D case to a shell-like problem. To simplify the full space flow to the in-plane flow, we introduce the planar projection tensor from the local monoclinic coordinates to project the flow onto the preform surface. Due to pressure different from the external environment and the flow, the fiber preform deformation and compaction are also interested. Based on the shell-like assumption, we propose a kinematic model to catch the normal directional stretch of the preform. We utilize the modified packing law in the linear momentum balance equation to obtain an ex-

plicit formation of the preform stretch. Thus the deformation will be illustrated by the stretch that only dependents on the mixture pressure from the homogenized flow. Given this simplification, we dramatically reduce the computational efforts but still can capture the central physics during the process. Also, the work is demonstrated through a mold filling process on the double curved thin-walled fiber preform, and the relevant swelling and the corresponding resin flow motion are observed from the numerical example.

5 Concluding remarks and future work

The present work contributes to the modeling of the liquid composite molding process. As the increasing demands on the composite materials, the manufacturers are facing the challenges from the request of high quality but low-cost manufacturing process. The old fashion and expensive prototype trails and errors procedure cannot bring enough competitiveness to manufacturers. Thus the numerical simulation tools are more important as ever nowadays. We provide the simulation tool to 1) improve the flow distribution arrangement; 2) controlling the injection time and pressure setting; 3) avoiding macro or microvoids; 4) predicting the thickness variations, spring-in, and spring-back; and the list goes on. We propose a novel model considering the capillary effect and extend Darcy's law to the gas-liquid homogenized flow. By virtue of the SUPG method, we present a panacea to solve the stability problem. Moreover, a kinematic assumption is made to describe the thin-walled FRPC components deformation during the infusion process. The explicit formulation of the preform stretch can illustrate the swelling and compaction behaviors of the fiber network. In view of the shell-like formulation, the full space model is reduced to in-plane flow embedded in the deformable shell preform. Regarding this simplification, the computational efforts are significantly reduced, and it proved the possibility to install this model in an optimization routine, which requires high computational efficiency.

From the simulation example in the **Paper A**, we notice that the flow velocity is not evenly distributed when the flow turns around a corner, which may lead to the local conversion. When the low-velocity flow settles, the resin starts to cure simultaneously. The consequence is then the resin properties, e.g., the viscosity will change, and consequently influences the infusion process. So it is essential to consider the local conversion in the model, e.g., utilized the Castro-Macosko model to reflect the viscosity of resin as a function of temperature and degree of cure [44]. Besides, it is also important to consider the influence of the temperature and heat transfer, since it highly relates to the resin viscosity and relevant permeability, e.g., [43]. In the current work, we only consider the isotropic permeability. However, due to the orientations of the fiber bundles, the FRPC materials usually have anisotropic permeability. Many researchers have developed different methods to measure or compute permeability, e.g., [33]. Furthermore, we have noticed that the saturation degree curves show a discontinuous jump at the flow fronts. This may give us hits to model the saturation degree based on a discontinuous method, e.g., Discontinuous Galerkin Method in [47]. On the other hand, the preform deformation model in the **Paper B** ignores the Euler rotation elemental wise. This assumption gives rise to nonconforming stretch fields. It is interesting to include the extra nodes in each element to represent the rotation and obtain the conforming stretch fields. Last but not least, experiments can be carried out to justify the accuracy of the models as future interests.

References

[1] S. G. Advani. *Flow and rheology in polymer composites manufacturing*. 10. Elsevier science, 1994.

[2] S. G. Advani and K.-T. Hsiao. *Manufacturing Techniques for Polymer Matrix Composites (PMCs)*. Elsevier, July 2012. ISBN: 978-0-85709-625-8.

[3] S. G. Advani and E. M. Sozer. *Process modeling in composites manufacturing*. CRC press, 2010.

[4] J. B. Alms, S. G. Advani, and J. L. Glancey. Liquid composite molding control methodologies using vacuum induced preform relaxation. *Composites Part A: Applied Science and Manufacturing* **42**.1 (2011), 57–65.

[5] B. T. Astrom. *Manufacturing of polymer composites*. CRC Press, 1997.

[6] C. Binetruy and S. G. Advani. Foam Core Deformation During Liquid Molding of Sandwich Structures: Modeling and Experimental Analysis. *Journal of Sandwich Structures & Materials* **5**.4 (Oct. 2003), 351–375. ISSN: 1099-6362. DOI: 10.1177/109963603027909.

[7] R. d. Boer. *Theory of Porous Media - Highlights in Historical Development | Reint de Boer | Springer*. 2000.

[8] R. M. Bowen. Incompressible porous media models by use of the theory of mixtures. *International Journal of Engineering Science* **18**.9 (1980), 1129–1148.

[9] R. M. Bowen. Compressible porous media models by use of the theory of mixtures. *International Journal of Engineering Science* **20**.6 (1982), 697–735.

[10] M. V. Bruschke and S. G. Advani. A finite element/control volume approach to mold filling in anisotropic porous media. *Polymer composites* **11**.6 (1990), 398–405.

[11] A. W. Chan and S.-T. Hwang. Modeling of the impregnation process during resin transfer molding. *Polymer Engineering & Science* **31**.15 (Aug. 1991), 1149–1156. ISSN: 1548-2634. DOI: 10.1002/pen.760311512.

[12] B. D. Coleman and W. Noll. The thermodynamics of elastic materials with heat conduction and viscosity. *Archive for rational mechanics and analysis* **13**.1 (1963), 167–178.

[13] S. Comas-Cardona, P. Groenenboom, C. Binetruy, and P. Krawczak. A generic mixed FE-SPH method to address hydro-mechanical coupling in liquid composite moulding processes. *Composites Part A: Applied Science and Manufacturing* **36**.7 (July 2005), 1004–1010. ISSN: 1359-835X. DOI: 10.1016/j.compositesa.2004.11.009.

[14] H. Darcy. *Les fontaines publiques de la ville de Dijon: exposition et application...* Victor Dalmont, 1856.

[15] R. S. Dave and A. C. Loos. *Processing of composites*. Hanser Publishers Munich, 2000.

[16] R. De Boer and W. Ehlers. The development of the concept of effective stresses. *Acta Mechanica* **83**.1-2 (1990), 77–92.

[17] M. Delesse. Pour déterminer la composition des roches. Annales des mines. *4. séries* **13** (1848), 379–388.

[18] W. Ehlers, T. Graf, and M. Ammann. Deformation and localization analysis of partially saturated soil. *Computer methods in applied mechanics and engineering* **193**.27-29 (2004), 2885–2910.

[19] L. Euler. Lettres á une Princesse d'Allemagne sur divers sujets de physique et de philosophie, Lettres, 2, L'Académie Impériale des Sciences de Saint-Pétersbourg, St. *Petersburg, Russia* (1768), 102–108.

[20] A. Fick. Ueber diffusion. *Annalen der Physik* **170**.1 (1855), 59–86.

[21] M. Goodman and S. Cowin. A continuum theory for granular materials. *Archive for Rational Mechanics and Analysis* **44**.4 (1972), 249–266.

[22] C. G. Grant, G. N. Bullen, A. Hiken, D. M. Champa, and D. Day. *Economics of Composites*. SAE International, Sept. 2015.

[23] W. G. Gray and S. M. Hassanizadeh. Paradoxes and Realities in Unsaturated Flow Theory. *Water Resources Research* **27**.8 (Aug. 1991), 1847–1854. ISSN: 1944-7973. DOI: 10.1029/91WR01259.

[24] W. G. Gray and C. T. Miller. *Introduction to the thermodynamically constrained averaging theory for porous medium systems*. Springer, 2014.

[25] T. G. P. Gutowski. *Advanced composites manufacturing*. John Wiley & Sons, 1997.

[26] S. V. Hoa. *Principles of the manufacturing of composite materials*. DEStech Publications, Inc, 2009.

[27] J. Larsson and R. Larsson. Non-linear analysis of nearly saturated porous media: theoretical and numerical formulation. *Computer Methods in Applied Mechanics and Engineering* **191**.36 (Aug. 2002), 3885–3907. ISSN: 0045-7825. DOI: 10.1016/S0045-7825(02)00333-X.

[28] R. Larsson, M. Rouhi, and M. Wysocki. Free surface flow and preform deformation in composites manufacturing based on porous media theory. *European Journal of Mechanics - A/Solids* **31**.1 (Jan. 2012), 1–12. ISSN: 0997-7538. DOI: 10.1016/j.euromechsol.2011.06.015.

[29] H.-S. Lee, H.-C. Sin, and S.-G. Kim. Iterative boundary pressure reflection method for the simulation of injection mold filling. *Polymer Engineering & Science* **30**.23 (Dec. 1990), 1513–1522. ISSN: 1548-2634. DOI: 10.1002/pen.760302305.

[30] R. W. Lewis, B. A. Schrefler, and N. A. Rahman. A finite element analysis of multiphase immiscible flow in deforming porous media for subsurface systems. *Communications in Numerical Methods in Engineering* **14**.2 (Feb. 1998), 135–149. ISSN: 1099-0887. DOI: 10.1002/(SICI)1099-0887(199802)14:2<135::AID-CNM134>3.0.CO;2-J.

[31] M. Li and C. L. Tucker. Modeling and simulation of two-dimensional consolidation for thermoset matrix composites. *Composites Part A: Applied Science and Manufacturing* **33**.6 (June 2002), 877–892. ISSN: 1359-835X. DOI: 10.1016/S1359-835X(02)00017-9.

[32] S. T. Lim and W. I. Lee. An analysis of the three-dimensional resin-transfer mold filling process. *Composites Science and Technology* **60**.7 (May 2000), 961–975. ISSN: 02663538. DOI: 10.1016/S0266-3538(99)00160-8.

[33] T. S. Lundström. The permeability of non-crimp stitched fabrics. *Composites Part A: Applied Science and Manufacturing* **31**.12 (Dec. 2000), 1345–1353. ISSN: 1359-835X. DOI: 10.1016/S1359-835X(00)00037-3.

[34] T. S. Lundström, R. Stenberg, R. Bergström, H. Partanen, and P. A. Birkeland. In-plane permeability measurements: a nordic round-robin study. *Composites Part A: Applied Science and Manufacturing* **31**.1 (Jan. 2000), 29–43. ISSN: 1359-835X. DOI: 10.1016/S1359-835X(99)00058-5.

[35] T. S. Lundström. Measurement of void collapse during resin transfer moulding. *Composites Part A: Applied Science and Manufacturing* **28**.3 (Jan. 1997), 201–214. ISSN: 1359-835X. DOI: 10.1016/S1359-835X(96)00109-1.

[36] T. S. Lundström and B. R. Gebart. Influence from process parameters on void formation in resin transfer molding. *Polymer Composites* **15**.1 (Feb. 1994), 25–33. ISSN: 1548-0569. DOI: 10.1002/pc.750150105.

[37] T. S. Lundström and B. R. Gebart. Effect of Perturbation of Fibre Architecture on Permeability Inside Fibre Tows. *Journal of Composite Materials* **29**.4 (Mar. 1995), 424–443. ISSN: 0021-9983. DOI: 10.1177/002199839502900401.

[38] T. S. Lundström, B. R. Gebart, and E. Sandlund. In-plane permeability measurements on fiber reinforcements by the multi-cavity parallel flow technique. *Polymer Composites* **20**.1 (Feb. 1999), 146–154. ISSN: 1548-0569. DOI: 10.1002/pc.10342.

[39] R. S. Maier, T. F. Rohaly, S. G. Advani, and K. D. Fickie. A Fast Numerical Method for Isothermal Resin Transfer Mold Filling. *International Journal for Numerical Methods in Engineering* **39**.8 (Apr. 1996), 1405–1417. ISSN: 1097-0207. DOI: 10.1002/(SICI)1097-0207(19960430)39:8<1405::AID-NME910>3.0.CO;2-S.

[40] M. A. Martínez, E. Cueto, M. Doblaré, and F. Chinesta. Natural element meshless simulation of flows involving short fiber suspensions. *Journal of Non-Newtonian Fluid Mechanics* **115**.1 (Oct. 2003), 51–78. ISSN: 0377-0257. DOI: 10.1016/S0377-0257(03)00171-X.

[41] B. Minaie, Y. F. Chen, and A. M. Mescher. A Methodology to Obtain a Desired Filling Pattern during Resin Transfer Molding. *Journal of Composite Materials* **36**.14 (July 2002), 1677–1692. ISSN: 0021-9983. DOI: 10.1177/0021998302036014165.

[42] L. Morland. A simple constitutive theory for a fluid-saturated porous solid. *Journal of geophysical research* **77**.5 (1972), 890–900.

[43] S. A. Niaki, A. Forghani, R. Vaziri, and A. Poursartip. A three-phase integrated flow-stress model for processing of composites. *Mechanics of Materials* **117** (Feb. 2018), 152–164. ISSN: 0167-6636. DOI: 10.1016/j.mechmat.2017.10.012.

[44] T. A. Osswald and G. Menges. *Materials science of polymers for engineers.* Carl Hanser Verlag GmbH Co KG, 2012.

[45] T. Papthanasiou and D. C. Guell. *Flow-induced alignment in composite materials.* Elsevier, 1997.

[46] S. L. Passman, J. W. Nunziato, and E. K. Walsh. "A theory of multiphase mixtures". *Rational thermodynamics.* Springer, 1984, pp. 286–325.

[47] J. Remacle, J. Flaherty, and M. Shephard. An Adaptive Discontinuous Galerkin Technique with an Orthogonal Basis Applied to Compressible Flow Problems. *SIAM Review* **45**.1 (Jan. 2003), 53–72. ISSN: 0036-1445. DOI: 10.1137/S00361445023830.

[48] M. S. Rouhi, M. Wysocki, and R. Larsson. Modeling of coupled dual-scale flow deformation processes in composites manufacturing. *Composites Part A: Applied*

Science and Manufacturing **46** (Mar. 2013), 108–116. ISSN: 1359-835X. DOI: 10.1016/j.compositesa.2012.11.002.

[49] J. Samir, J. Echaabi, and M. Hattabi. Numerical algorithm and adaptive meshing for simulation the effect of variation thickness in resin transfer molding process. *Composites Part B-Engineering* **42**.5 (July 2011), 1015–1028. ISSN: 1359-8368. DOI: 10.1016/j.compositesb.2011.03.027.

[50] M. Sawley, P. Cleary, and J. Ha. Modelling of flow in porous media and resin transfer moulding using smoothed particle hydrodynamics (1999).

[51] W. H. Seemann III. *Plastic transfer molding techniques for the production of fiber reinforced plastic structures.* Google Patents, Feb. 1990.

[52] W. H. Seemann. *Plastic transfer molding apparatus for the production of fiber reinforced plastic structures.* Google Patents, Oct. 1991.

[53] S. Soukane and F. Trochu. Application of the level set method to the simulation of resin transfer molding. *Composites Science and Technology* **66**.7 (June 2006), 1067–1080. ISSN: 0266-3538. DOI: 10.1016/j.compscitech.2005.03.001.

[54] J. Stefan. *Über das Gleichgewicht und die Bewegung, insbesondere die Diffusion von Gasgemengen.* Universitätsbibliothek Johann Christian Senckenberg, 2007.

[55] A. B. Strong. *Fundamentals of composites manufacturing: materials, methods and applications.* Society of Manufacturing Engineers, 2008.

[56] A. Szymkiewicz. *Mathematical Models of Flow in Porous Media.* GeoPlanet: Earth and Planetary Sciences. Springer Berlin Heidelberg, 2013. ISBN: 978-3-642-23558-0 978-3-642-23559-7. DOI: 10.1007/978-3-642-23559-7_2.

[57] S. Toll. Packing mechanics of fiber reinforcements. *Polymer Engineering & Science* **38**.8 (Aug. 1998), 1337–1350. ISSN: 1548-2634. DOI: 10.1002/pen.10304.

[58] F. Trochu, R. Gauvin, and D.-M. Gao. Numerical analysis of the resin transfer molding process by the finite element method. *Advances in Polymer Technology* **12**.4 (Dec. 1993), 329–342. ISSN: 1098-2329. DOI: 10.1002/adv.1993.060120401.

[59] M.-K. Um and W. I. Lee. A study on the mold filling process in resin transfer molding. *Polymer Engineering & Science* **31**.11 (June 1991), 765–771. ISSN: 1548-2634. DOI: 10.1002/pen.760311102.

[60] J. Varna, R. Joffe, L. A. Berglund, and T. S. Lundström. Effect of voids on failure mechanisms in RTM laminates. *Composites Science and Technology.* Mesostructures and Mesomechanics in Fibre Composites **53**.2 (Jan. 1995), 241–249. ISSN: 0266-3538. DOI: 10.1016/0266-3538(95)00024-0.

[61] V. R. Voller and Y. F. Chen. Prediction of Filling Times of Porous Cavities. *International Journal for Numerical Methods in Fluids* **23**.7 (Oct. 1996), 661–672. ISSN: 1097-0363. DOI: 10.1002/(SICI)1097-0363(19961015)23:7<661::AID-FLD448>3.0.CO;2-E.

[62] V. R. Voller and S. Peng. An algorithm for analysis of polymer filling of molds. *Polymer Engineering & Science* **35**.22 (Nov. 1995), 1758–1765. ISSN: 1548-2634. DOI: 10.1002/pen.760352205.

[63] R. Woltmann. *Beitrage zur Hydraulischen architectur.* Johann Christian Dieterich, 1794.

[64] D. Wu and R. Larsson. Homogenized free surface flow in porous media for wet-out processing. *International Journal for Numerical Methods in Engineering* **1**.17 (May 2018). ISSN: 00295981. DOI: 10.1002/nme.5812.

[65] M. Wysocki, L. E. Asp, S. Toll, and R. Larsson. Two phase continuum modelling of composites consolidation. *Plastics, Rubber and Composites* **38**.2-4 (May 2009), 93–97. ISSN: 1465-8011. DOI: 10.1179/174328909X387856.

[66] M. Wysocki, R. Larsson, and S. Toll. Hydrostatic consolidation of commingled fibre composites. *Composites Science and Technology* **65**.10 (Aug. 2005), 1507–1519. ISSN: 0266-3538. DOI: 10.1016/j.compscitech.2005.01.002.

[67] M. Wysocki, S. Toll, R. Larsson, and L. E. Asp. Anisotropic and tension compression asymmetric model for composites consolidation. *Composites Part A: Applied Science and Manufacturing* **41**.2 (Feb. 2010), 284–294. ISSN: 1359-835X. DOI: 10.1016/j.compositesa.2009.10.016.

[68] B. Yang, T. Jin, J. Li, and F. Bi. Simulating the resin flow and stress distributions on mold tools during compression resin transfer molding. *Journal of Reinforced Plastics and Composites* **33**.14 (July 2014), 1316–1331. ISSN: 0731-6844. DOI: 10.1177/0731684414528831.

[69] W. B. Young, K. H. L. H. Fong, and L. J. Lee. Flow simulation in molds with preplaced fiber mats. *Polymer Composites* **12**.6 (Dec. 1991), 391–403. ISSN: 1548-0569. DOI: 10.1002/pc.750120604.

[70] W. B. Young, K. Rupel, K. Han, L. J. Lee, and M. J. Liou. Analysis of resin injection molding in molds with preplaced fiber mats. II: Numerical simulation and experiments of mold filling. *Polymer Composites* **12**.1 (Feb. 1991), 30–38. ISSN: 1548-0569. DOI: 10.1002/pc.750120106.